COUPLED WATER TRANSPORT IN STANDING GRADIENT MODELS OF THE LATERAL INTERCELLULAR SPACE

ALAN M. WEINSTEIN AND JOHN L. STEPHENSON, *Section on Theoretical Biophysics, National Heart, Lung and Blood Institute and Mathematical Research Branch, National Institute of Arthritis, Metabolism and Digestive Diseases, National Institutes of Health, Bethesda, Maryland 20205 U.S.A.*

ABSTRACT A standing gradient model of the lateral intercellular space is presented which includes a basement membrane of finite solute permeability. The solution to the model equations is estimated analytically using the "isotonic convection approximation" of Segel. In the case of solute pumps uniformly distributed along the length of the channel, the achievement of isotonic transport depends only on the water permeability of the cell membranes. The ability of the model to transport water against an adverse osmotic gradient is the sum of two terms: The first term is simply that for a well-stirred compartment model and reflects basement membrane solute permeability. The second term measures the added strength due to diffusion limitation within the interspace. It is observed, however, that the ability for uphill water transport due to diffusion limitation is diminished by high cell membrane water permeability. For physiologically relevant parameters, it appears that the high water permeability required for isotonic transport renders the contribution of the standing gradient relatively ineffective in transport against an osmotic gradient. Finally, when the model transports both isotonically and against a gradient, it is shown that substantial intraepithelial solute polarization effects are unavoidable. Thus, the measured epithelial water permeability will grossly underestimate the water permeability of the cell membranes. The accuracy of the analytic approximation is demonstrated by numerical solution of the complete model equations.

INTRODUCTION

Models of epithelial transport of water have been developed to elucidate the mechanisms of "uphill transport" and "isotonic transport." Uphill transport denotes the ability of an epithelium to transport water against an adverse osmotic gradient. Isotonic transport refers to observations made in two experimental settings in which initially identical solutions bathe the mucosal and serosal surfaces of the tissue. In one case, the mucosal bath is small relative to the serosal bath; in the second case the serosal bath is relatively small or is, in fact, generated by the transported salt solution. In either case, as transport proceeds over time, the osmolalities on either side of the epithelium tend toward definite limiting values. Isotonic transport signifies that these limiting values are little different from the initial, or reference, osmolality.

Since the work of Curran and Solomon (1957), both uphill and isotonic transport have been viewed in terms of the "coupling" of transepithelial water flow to metabolically driven solute flux. Curran (1960) speculated that the mechanism of such coupling was the transport of salt into a well-stirred intraepithelial compartment, such as the lateral intercellular space. A small increment in the osmolality of this compartment above that of the mucosal bath produces osmotic water flow across the cell membranes into the interspace. This results in an increase in hydrostatic pressure within the interspace and thus convective flow of the channel contents across the channel basement membrane and into the serosal bath. The intuitive appeal of this scheme to represent uphill transport was strengthened by the actual construction of an analogous macroscopic system and the observation of its functioning as predicted (Curran and MacIntosh, 1962; Ogilvie et al., 1963).

However, the capability of such a model to adequately simulate isotonic transport by rabbit gallbladder epithelium was seriously questioned by Diamond (1964 *b*). In an effort to repair this difficulty while preserving the basic idea of the middle compartment scheme, Diamond and Bossert (1967) lifted the assumption that the lateral interspace was well stirred. In their "standing gradient" model, the flow of solute and volume along the length of the paracellular channel is described by the diffusion equation. Solute input occurs largely in an apical region of the channel and as flow proceeds toward the channel mouth there is osmotic equilibration of the channel contents with the cell interior. Numerical calculations revealed that this equilibration was enhanced by a small diffusion coefficient or a small channel radius or by a large cell membrane water permeability or a long channel length. Equilibration was quite independent of total solute transport rate but was impaired substantially as solute transport was permitted along the whole channel length. The differential equation of Diamond and Bossert was studied by Segel (1970), who presented an approximate solution to the model equation, and confirmed analytically the previous numerical results.

Nevertheless, the standing gradient model has received a certain measure of criticism. One objection has been that the parameters necessary to achieve full equilibration are not physiologically realistic (Hill, 1975, 1977; Hill and Hill, 1978). However, the validity of Hill's own parameter choices has been disputed (Diamond, 1978, 1979). The localization of solute pumps to the channel apex has also been criticized. Localization studies of the putative solute pump along the lateral cell membranes, $Na^+ - K^+$ ATPase, have all shown a uniform pump distribution (Stirling, 1972; Kyte, 1976; DiBona and Mills, 1979). Finally, and perhaps the most subtle of the "difficulties" of standing gradient theory, has been the observation that when channel models are solved for the case of identical bathing media and uniform solute pumping, no significant standing gradients are observed (Sackin and Boulpaep, 1975; Huss and Marsh, 1975; Weinstein and Stephenson, 1979).

Recently, we have discussed the problem of modeling epithelial solute-solvent coupling and presented a systematic and general framework for the assessment of such models.[1] In part, the view presented was that at least some of the controversy surrounding the simulation of coupled water transport has derived from incomplete series of model calculations, rather than model inadequacy. It has been indicated that a minimum set of necessary calculations includes: (*a*) an estimate of the strength of transport of the model; (*b*) verification of transport isotonicity; and (*c*) evaluation of the effective water permeability of the model. Estimation of strength of transport means the simulation of steady-state experiments in which the mucosal bath is made

[1]Weinstein, A. M., and J. L. Stephenson. 1980. Models of coupled salt and water transport across leaky epithelia. *J. Membr. Biol.* In press.

progressively hypertonic until mucosal-to-serosal volume flow is just nullified. As in the experimental setting, the verification of transport isotonicity for an epithelial model requires two sets of calculations: In one case the serosa is held fixed at the reference and the osmolality of the mucosal bath is determined which will exactly equal the osmolality of the transported solution. This is the condition of mucosal transport equilibrium. In the second case, the mucosa is held at the reference and one solves for the serosal osmolality which yields serosal transport equilibrium. In the case of isotonic transport these two equilibrium osmolalities will differ minimally from reference. Finally, the effective water permeability of the model is found by calculating the effect on transepithelial volume flow produced by the addition of an impermeant species to one of the bathing media.

With this scheme, we reconsidered the well-stirred compartment model of the lateral intercellular space, and indicated that this type of model could adequately represent a rabbit gallbladder epithelium.[1] In particular, it was observed that the osmotic deviation relevant to the verification of isotonic transport depended only on the high water permeability of the cell membranes. Nevertheless, the observed water permeability of the epithelium was substantially less than these cell membrane permeabilities due to intraepithelial solute polarization effects (caused by the finite solute permeability of the channel basement membrane). For such a compartment model that could transport both against a substantial gradient, as well as isotonically, it was shown that significant intraepithelial polarization effects are inescapable.

In the present manuscript we first review the general plan of the calculations for an epithelial model when the transepithelial fluxes are written (abstractly) as functions of the bathing solution osmolalities. For the case that these fluxes may be approximated by a particularly simple pair of linear equations, these calculations are carried out analytically. This has the advantage of being able to relate the osmotic coupling coefficient of the model to strength of transport and isotonicity in a manner that is independent of the particular details of model construction. Once the standing gradient model of section two has been cast into this linear form, its analysis is, in a sense, already completed.

In section two, a standing gradient model of the lateral intercellular space is presented which differs from the original Diamond and Bossert model only in the inclusion of a basement membrane of finite solute permeability. The model is then brought into a linear form using the isotonic convection approximation of Segel (1970). From this analysis it is shown that the strength of transport is the sum of two terms: The first is precisely that found for the well-stirred compartment model and reflects the solute permeability of the basement membrane; the second term appears as a result of the diffusion limitation within the interspace. It will be an important observation that the magnitude of this second term is diminished by high cell membrane water permeability. For the standing gradient model, as in the compartment model, transport isotonicity depends only on the cell membrane water permeability and is independent of any diffusion limitation. Finally, significant solute polarization effects will be shown to be an inescapable feature of this model when the parameters are such as to permit both uphill and isotonic transport.

In the last section, the model calculations will be illustrated using a set of parameters suggestive of rabbit gallbladder epithelium. Several additional parameter sets will also be employed to gain a sense of the dependence of model performance on the parameter choice. With these parameter sets, the accuracy of the isotonic convection approximation in these calculations will be demonstrated. Further, these numerical examples will suggest that the high cell membrane water permeabilities required for isotonic transport will result in only a small contribution by the interspace itself to the strength of transport.

THE ANALYSIS OF A MODEL OF COUPLED WATER TRANSPORT

Denote by J_v the transepithelial volume flow, and by J_s the transepithelial solute flux. One may write formal steady-state relations for these flows,

$$J_v = J_v(C_M, C_S; C_O)$$
$$J_s = J_s(C_M, C_S; C_O), \tag{1-1}$$

where C_O is the reference osmolality and C_M and C_S are the deviations from reference of the mucosal and serosal bathing solutions. Eq. 1-1 apply to a large variety of models and implicit in this formulation is the condition of equal hydrostatic pressures within each bath. Specifically, this general formulation permits us to consider models in which the transepithelial flow of salt and water are, in part, metabolically driven and may occur between identical bathing solutions.

For this model, the strength of transport, $\hat{C}$, is defined as the solution to the equation

$$J_v(\hat{C}, O; C_O) = 0. \tag{1-2}$$

That is, $\hat{C}$ is the increase above reference of the mucosal bath osmolality that is required to null transepithelial volume flow. For any bath conditions, the concentration of the transported solution is defined by

$$C_R(C_M, C_S; C_O) = \frac{J_s}{J_v}. \tag{1-3}$$

Thus, the condition of mucosal bath transport equilibrium is represented by the equation

$$C_R(C_M^*, O; C_O) = C_O + C_M^*, \tag{1-4}$$

which states that the osmolality of the transported solution is precisely that of the mucosal bath. Similarly, serosal transport equilibrium is determined by solving

$$C_R(O, C_S^*; C_O) = C_O + C_S^*. \tag{1-5}$$

From this perspective, isotonic transport means that the concentrations, C_M^* and C_S^*, which satisfy Eqs. 1-4 and 1-5, are at most a few percent of C_O.

This solution of Eqs. 1-4 and 1-5 is a different task from the simple determination of the reabsorbate osmolality for identical bathing media, $C_R(O, O; C_O)$. In the case of equal bathing media we shall adopt the notation

$$(J_v)_O = J_v(O, O; C_O)$$
$$(J_s)_O = J_s(O, O; C_O)$$
$$(C_R)_O = C_R(O, O; C_O) = \frac{(J_s)_O}{(J_v)_O}. \tag{1-6}$$

The reference state transport tonicity, $(C_R)_O$, is, nevertheless, an important theoretical aspect of model performance and has been used to define the coupling coefficient of osmotic transport[1] by

$$\gamma = \frac{C_O}{(C_R)_O} = \frac{(J_v)_O}{(J_s)_O/C_O}. \tag{1-7}$$

Thus, the osmotic coupling coefficient is the ratio of the actual volume flow observed with equal bathing media relative to the virtual volume flow that would be necessary for absorption to be isotonic, $(J_s)_O/C_O$. For tight coupling, $\gamma \approx 1$; in an uncoupled system $\gamma = 0$. γ has also been termed the efficiency of osmotic transport (Hill and Hill, 1978).

Many of the important aspects of coupled water transport may be appreciated by studying the linear model that best approximates Eqs. 1-1 near the reference state. This is given by the Taylor series

$$\begin{aligned} J_v &= (J_v)_O + \left(\frac{\partial J_v}{\partial C_M}\right)_O C_M + \left(\frac{\partial J_v}{\partial C_S}\right)_O C_S \\ J_s &= (J_s)_O + \left(\frac{\partial J_s}{\partial C_M}\right)_O C_M + \left(\frac{\partial J_s}{\partial C_S}\right)_O C_S. \end{aligned} \tag{1-8}$$

In the approximate standing gradient model that we shall consider, rectification will be absent. (In rabbit gallbladder, this is supported by observations of Diamond, 1966.) This means that the observed permeabilities are independent of the direction of the imposed gradient, and this implies

$$\left(\frac{\partial J_v}{\partial C_M}\right)_O = -\left(\frac{\partial J_v}{\partial C_S}\right)_O \text{ and } \left(\frac{\partial J_s}{\partial C_M}\right)_O = -\left(\frac{\partial J_s}{\partial C_S}\right)_O. \tag{1-9}$$

Further, the transepithelial salt flux will be independent of deviations in the bath osmolalities, or

$$\left(\frac{\partial J_s}{\partial C_M}\right)_O = \left(\frac{\partial J_s}{\partial C_S}\right)_O = 0. \tag{1-10}$$

(Some experimental support for this insensitivity of salt flux to salt concentration may be found in the observations of Whitlock and Wheeler [1964] on rabbit gallbladder.) Thus, the approximate standing gradient model will take the form

$$\begin{aligned} J_v &= (J_v)_O + \left(\frac{\partial J_v}{\partial C_M}\right)_O (C_M - C_S) \\ J_s &= (J_s)_O. \end{aligned} \tag{1-11}$$

For a model given by Eqs. 1-11, the strength of transport is

$$\hat{C} = -(J_v)_O/\left(\frac{\partial J_v}{\partial C_M}\right)_O, \tag{1-12}$$

and the tonicity of the transported solution is

$$C_R = \frac{C_O}{\gamma}\left[1 - \frac{C_M - C_S}{\hat{C}}\right]^{-1}. \tag{1-13}$$

The Eqs. 1-4 and 1-5 that are used to determine the conditions of transport equilibrium may now be written

$$C_O + C_M^* = \frac{C_O}{\gamma}\left[1 - \frac{C_M^*}{\hat{C}}\right]^{-1}. \tag{1-14}$$

$$C_O + C_S^* = \frac{C_O}{\gamma}\left[1 + \frac{C_S^*}{\hat{C}}\right]^{-1}. \tag{1-15}$$

Eqs. 1-14 and 1-15 are quadratic in the osmotic deviations C_M^* and C_S^*, but in the case that the model can transport both isotonically and against a substantial gradient they have the approximate solutions[2]

$$-C_M^* \approx \hat{C}(\frac{1}{\gamma} - 1)/(1 - \hat{C}/C_O) \tag{1-16}$$

$$C_S^* \approx \hat{C}(\frac{1}{\gamma} - 1)/(1 + \hat{C}/C_O) \tag{1-17}$$

It is useful to observe that in the examples of interest the magnitude of C_M^* and C_S^* is determined by the numerator of Eqs. 1-16 and 1-17 which will be written

$$C^* = \hat{C}\left(\frac{1}{\gamma} - 1\right). \tag{1-18}$$

(That is, for a rabbit gallbladder capable of transporting against 80 mosmol/liter $\hat{C}/C_O$ = 0.27 and denominators of Eqs. 1-16 and 1-17 are close to 1.) This quantity satisfies the equation

$$C_R(-C^*, O) = C_R(O, C^*) = C_O, \tag{1-19}$$

and is the osmotic deviation required to obtain the transport tonicity at precisely the reference osmolality. Inspection of Eq. 1-18 reveals that for the epithelium, the capability of isotonic transport and of significant uphill transport, taken together, implies that coupling is tight ($\gamma \approx 1$).

It is important to make the observation that for this model, (where the reflection coefficient is 1), the measured epithelial water permeability, $L_{P,\text{obs}}$, is

$$RTL_{P,\text{obs}} = -\left(\frac{\partial J_v}{\partial C_M}\right)_O. \tag{1-20}$$

[2] C_M^* satisfies: $C_M^*[1 - \hat{C}/C_O + C_M^*/C_O] = \hat{C}(1/\gamma - 1)$, so that for $C_M^*/\hat{C} \ll 1$, we obtain Eq. 1-16.

Thus, the strength of coupled transport given in Eq. 1-12 may be written

$$\hat{C} = \frac{[(J_s)_O/C_O]\gamma}{L_{P,\mathrm{obs}}}, \tag{1-21}$$

where the coupled water flow, $(J_v)_O$, has been replaced according to Eq. 1-7. Finally, substitution of Eq. 1-21 into Eq. 1-18 yields

$$C^* = \frac{[(J_s)_O/C_O](1-\gamma)}{L_{P,\mathrm{obs}}}, \tag{1-22}$$

The numerator of Eq. 1-22 identifies a "noncoupled" fraction of the water flow required for isotonicity. It is this aliquot that must be driven by the establishment of a transepithelial osmotic gradient. Recall, however, that in many tissues this transepithelial osmotic gradient may be a negligible fraction of the reference osmolality (<2%) and thus these tissues are said to transport "isotonically."

A STANDING GRADIENT MODEL OF THE LATERAL INTERCELLULAR SPACE

The model of Diamond and Bossert (1967) supposes a channel of length L, cross section area A, and circumference S (Fig. 1). Distance along the channel, x, is measured from the tight junction ($x = 0$) to the channel mouth ($x = L$). The cell is at the mucosal bath osmolality, $C_O + C_M$, and the serosal bath is at $C_O + C_S$. The lateral cell membrane has unit water permeability RTL_p (cm/s·osmol) and transports solute into the interspace at rate $N(x)$ (mosmol/cm^{2}s). The solute transport rate is written as a function of position because in the model, solute transport is assumed to occur only in an apical segment of the channel. In this apical segment, transport, N, is constant. If λ is the fraction of channel length over which solute transport occurs, then

$$J_s = J_s(L) = \lambda LSN \tag{2-1}$$

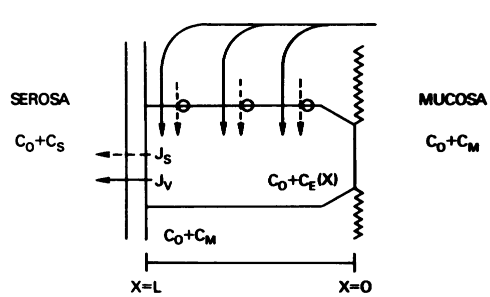

FIGURE 1 Schematic representation of the lateral intercellular space. The channel is assumed sealed at the apex and bounded at the base by a membrane of finite solute permeability. There is solute input across the cell membrane along a specified (apical) fraction of the channel length. The cell and mucosal medium are assumed to be at the same osmolality.

is the total transepithelial solute flux. The model variables are the channel concentration, $C_O + C_E(x)$, volume flow, $J_v(x)$, and solute flux $J_s(x)$.

The solute flux in the channel is written as a sum of convective and diffusive terms in the equation

$$J_s = [J_v(C_O + C_E)] - DA\frac{dC_E}{dx}. \tag{2-2}$$

The model equations are completed by specifying the steady-state mass conservation relations for volume

$$\frac{dJ_v}{dx} = S\,RTL_P(C_E - C_M), \tag{2-3}$$

and solute

$$\frac{dJ_s}{dx} = SN(x). \tag{2-4}$$

The system of three first-order Eqs., 2-2–2-4, requires three boundary conditions. In the original standing gradient model, (Diamond and Bossert, 1967) the boundary data were those for a sealed tight junction,

$$J_v(O) = 0 \tag{2-5}$$

$$J_s(O) = 0, \tag{2-6}$$

and for the channel opening directly into the serosal bath,

$$C_E(L) - C_S = 0. \tag{2-7}$$

In the present analysis, the condition of a sealed tight junction is retained but the problem has been expanded to include a channel basement membrane of finite solute permeability. For this problem, the boundary condition at $x = L$ is

$$J_v(L)\,(C_O + C_B) + H_B[C_E(L) - C_S] = J_s(L) \tag{2-8}$$

where

$$C_O + C_B = C_O + \frac{1}{2}(C_E(L) + C_S)$$

is the mean osmolality of the barrier separating the channel mouth from the serosal bath and $H_B(\text{cm}^3/\text{s})$ is the solute permeability of this barrier.

Considerable insight has been gained into the performance of the standing gradient model from the analytical treatment of Segel (1970) (see also Lin and Segel, 1974). Segel found that for the problem with boundary conditions Eqs. 2-5–2-7, little accuracy was lost by approximating the diffusion Eq. 2-2 by

$$J_s = J_vC_O - DA\frac{dC_E}{dx}. \tag{2-9}$$

Weinstein and Stephenson[1] have shown that this "isotonic convection approximation" can also be applied to simplify the boundary condition in Eq. 2-8 to

$$J_v(L)\, C_O + H_B[C_E(L) - C_S] = J_s(L). \tag{2-10}$$

With these simplifications, the differential Eqs. 2-3, 2-4, and 2-9 along with the boundary data in Eqs. 2-5, 2-6, and 2-10 constitute a linear model of the lateral intercellular space. Clearly, these approximations will be accurate only for the cases in which C_M, C_S, and $C_E(x)$ are small relative to the reference, C_O. That these cases include examples of physiological interest will be demonstrated in the model calculations of the following section. The remainder of this section will be devoted to the analysis of this linear approximate model.

It will be convenient to introduce the notation

$$\pi = \sqrt{SL\, RTL_pC_O} \tag{2-11}$$

$$\delta = \sqrt{\frac{DA}{L}} \tag{2-12}$$

and, following Segel,

$$\mathrm{K} = \frac{\pi}{\delta} = \sqrt{\frac{SL^2RTL_pC_O}{DA}}\,. \tag{2-13}$$

Then, differentiating Eq. 2-9 with respect to x, and substituting Eqs. 2-3 and 2-4 for the flux derivatives one obtains

$$\frac{d^2C_E}{dx^2} = \left(\frac{K}{L}\right)^2 (C_E - C_M) - \frac{SN(x)}{L\delta^2}, \tag{2-14}$$

where $N(x)$ is either constant or zero and satisfies Eq. 2-1. The conditions of Eqs. 2-5 and 2-6, along with Eq. 2-9, require that at $x = 0$,

$$\frac{dC_E}{dx}(O) = 0. \tag{2-15}$$

Given $C_E(x)$, Eq. 2-3 is integrated along the length of the channel to obtain the transepithelial volume flow

$$J_v = J_v(L) = \int_O^L S\, RTL_P(C_E - C_M)\, dx. \tag{2-16}$$

Thus, the boundary relation in Eq. 2-10 may be rewritten

$$\frac{\pi^2}{L}\int_O^L (C_E - C_M)\, dx + H_B(C_E(L) - C_s) = J_s. \tag{2-17}$$

The solution to Eq. 2-14 for the apical and basal segments of the channel may be written

$$C_E(x) - C_M = A_{11}\cosh\left(\frac{Kx}{L}\right) + A_{12}\sinh\left(\frac{Kx}{L}\right) + \frac{J_s}{\lambda\pi^2} \quad 0 \le x \le \lambda L \tag{2-18}$$

and

$$C_E(x) - C_M = A_{21}\cosh\left(\frac{Kx}{L}\right) + A_{22}\sinh\left(\frac{Kx}{L}\right) \quad \lambda L \le x \le L. \tag{2-19}$$

The coefficients A_{ij} are determined so as to satisfy the two boundary conditions in Eqs. 2-15 and 2-17, as well a to match $C_E(x)$ and dC_E/dx at the point $x = \lambda L$. Thus, Eqs. 2-18 and 2-19 become

$$C_E(x) - C_M = \left(\frac{J_s}{\lambda\pi^2}\left\{\sinh(K\lambda)\left[\frac{\frac{\delta\pi}{H_B}\cosh(K) + \sinh(K)}{\cosh(K) + \frac{\delta\pi}{H_B}\sinh(K)}\right] - \cosh(K\lambda)\right\} + \frac{C_S - C_M}{\cosh(K) + \frac{\delta\pi}{H_B}\sinh(K)}\right)\cosh\left(\frac{Kx}{L}\right) + \frac{J_s}{\lambda\pi^2} \quad 0 \le x \le \lambda L \tag{2-20}$$

and

$$C_E(x) - C_M = \left(\frac{J_s}{\lambda\pi^2}\sinh(K\lambda)\left[\frac{\frac{\delta\pi}{H_B}\cosh(K) + \sinh(K)}{\cosh(K) + \frac{\delta\pi}{H_B}\sinh(K)}\right] + \frac{C_S - C_M}{\cosh(K) + \frac{\delta\pi}{H_B}\sinh(K)}\right)\cosh\left(\frac{Kx}{L}\right) - \frac{J_s}{\lambda\pi^2}\sinh(K\lambda)\sinh\left(\frac{Kx}{L}\right) \quad \lambda L \le x \le L.^3 \tag{2-21}$$

Eqs. 2-20 and 2-21 are used to evaluate the transepithelial volume flow according to Eq. 2-16:

$$J_v = \frac{J_s}{C_O}\left\{1 - \frac{\sinh(K\lambda)}{K\lambda\left[\cosh(K) + \frac{\delta\pi}{H_B}\sinh(K)\right]}\right\} + \frac{\delta\pi}{C_O}\frac{\sinh(K)(C_S - C_M)}{\cosh(K) + \frac{\delta\pi}{H_B}\sinh(K)}. \tag{2-22}$$

[3]For the purpose of numerical calculation it is useful to note that Eq. 2-20 may be rewritten

$$C_E(x) - C_M = \left(\frac{J_s}{\lambda\pi^2}\left\{\frac{\frac{\delta\pi}{H_B}\sinh(K(\lambda - 1)) - \cosh(K(\lambda - 1))}{\cosh(K) + \frac{\delta\pi}{H_B}\sinh(K)}\right\} + \frac{C_S - C_M}{\cosh(K) + \frac{\delta\pi}{H_B}\sinh(K)}\right)\cosh\left(\frac{Kx}{L}\right) + \frac{J_s}{\lambda\pi^2} \quad 0 \le x \le \lambda L,$$

For the case considered by Segel (1970), $C_S - C_M = 0$ and $H_B \rightarrow \infty$, the expression for J_v in Eq. 2-22 reduces to his more familiar formula

$$J_v = \frac{J_s}{C_O}\left[1 - \frac{\sinh(K\lambda)}{K\lambda \cosh(K)}\right]. \tag{2-23}$$

Together the Eqs. 2-22 and 2-1 constitute a linear model of the form in Eq. 1-11, and the analysis given for that system may now be applied.

The osmotic coupling coefficient for this model is

$$\gamma = \frac{(J_v)_O C_O}{(J_s)_O} = 1 - \left[\frac{K\lambda \cosh(K)}{\sinh(K\lambda)} + \frac{\pi^2}{H_B}\frac{\lambda \sinh(K)}{\sinh(K\lambda)}\right]^{-1} \tag{2-24}$$

and for the case of uniform solute input along the length of the channel, ($\lambda = 1$),

$$\gamma = 1 - \left[\frac{K}{\tanh(K)} + \frac{\pi^2}{H_B}\right]^{-1}. \tag{2-25}$$

According to Eqs. 2-24 or 2-25, coupling will be tight whenever either of the two terms within the brackets is large. When the second of these terms dominates, the model is essentially a compartment model and the coupling coefficient is akin to that computed by Weinstein and Stephenson.[1] The first term can dominate when K is large. This means that the primary locus of osmotic coupling is within the channel and this will be the case for either a small diffusion coefficient, $\delta = \sqrt{DA/L}$, or a high cell membrane water permeabilty, $\pi = \sqrt{SLRTL_pC_O}$.

The strength of transport of the model is

$$\hat{C} = \frac{J_s}{H_B} + \frac{J_s}{\delta\pi}\left[\frac{1}{\tanh(K)} - \frac{\sinh(K\lambda)}{K\lambda \sinh(K)}\right], \tag{2-26}$$

and for the case of uniform solute input, ($\lambda = 1$),

$$\hat{C} = \frac{J_s}{H_B} + \frac{J_s}{\delta\pi}\left[\frac{1}{\tanh(K)} - \frac{1}{K}\right]. \tag{2-27}$$

The first term in Eq. 2-26 is precisely the strength of transport obtained for the elementary compartment model of the lateral intercellular space.[1] The strength of transport for the well-stirred compartment is limited by the rate of solute escape across the basement

---

and Eq. 2-21 may be rewritten

$$C_E(x) - C_M = \frac{J_s}{\lambda\pi^2}\sinh(K\lambda)\left\{\frac{\sinh\left[K\left(1 - \frac{x}{L}\right)\right] + \frac{\delta\pi}{H_B}\cosh\left[K\left(1 - \frac{x}{L}\right)\right]}{\cosh(K) + \frac{\delta\pi}{H_B}\sinh(K)}\right\}$$

$$+ \frac{C_S - C_M}{\cosh(K) + \frac{\delta\pi}{H_B}\sinh(K)}\cosh\left(\frac{Kx}{L}\right) \quad \lambda L \le x \le L.$$

membrane. The second term represents the strength of transport due to diffusion limitation within the interspace. This term is always less than $J_s/\delta\pi$ and will approach this value for tight coupling within the channel ($K > 5$). It should be observed that when K is large due to a small value of δ, the diffusion limitation is greater so that the strength of transport is enhanced. However, when coupling is tight due to high cell membrane, water permeability, π, the strength of transport is diminished. As will be illustrated in the next section, this last observation may be rationalized by noting that for larger values of π there is greater interspace convective flow, and hence mixing of the channel contents.

The osmotic deviation pertinent to isotonic transport may be obtained by substitution of Eqs. 2-24 and 2-26 into Eq. 1-18. Thus,

$$C^* = \frac{J_s}{\lambda \pi^2} \frac{\sinh(K\lambda)}{\sinh(K)} \leq \frac{J_s}{\pi^2} \tag{2-28}$$

and when solute transport is uniform

$$C^* = \frac{J_s}{\pi^2} = \frac{J_s}{SLRTL_PC_O}. \tag{2-29}$$

These results carry the strong implication that transport isotonicity is determined almost solely by the water permeability of the cell membranes. It is largely independent of the effect of a finite basement membrane solute permeability or of diffusion limitation within the channel (at least for uniform pump distribution). It is of interest to note that the expression in Eq. 2-29 is precisely what one would write for a simple membrane between two well-stirred bathing solutions.

One of the important features, however, that distinguishes the interspace model from a simple membrane is that the water permeability that is measured by the imposition of an osmotic gradient, $L_{P,\text{obs}}$, is different from the L_P that is relevant to transport isotonicity. This discrepancy is commonly referred to as "intraepithelial solute polarization effect." Eq. 2-22 permits us to determine the measured water permeability according to Eq. 1-20 so that

$$RT\, L_{P,\text{obs}} = \frac{\pi^2}{C_O} \frac{\lambda \sinh(K)}{\sinh(K\lambda)} (1 - \gamma) \tag{2-30}$$

or when $\lambda = 1$

$$RTL_{P,\text{obs}} = \frac{\pi^2}{C_O}(1 - \gamma) = SLRTL_P(1 - \gamma). \tag{2-31}$$

Thus, the solute polarization effect is an inescapable feature of coupled water transport in this interspace model. Tight coupling will vitiate any attempt to use the measured epithelial water permeability as an estimate for the membrane permeability that is pertinent to isotonic transport.

Finally, one may address the problem of the existence of "standing" osmotic gradients along the length of the interspace by evaluating Eq. 2-20 at $x = 0$ and Eq. 2-21 at $x = L$. Subtracting these two expressions, one finds

$C_E(O) - C_E(L)$

$$= \frac{J_s}{\lambda\pi^2}\left\{1 - \frac{\frac{\delta\pi}{H_B}\sinh(K\lambda) + \frac{\delta\pi}{H_B}\sinh[K(1-\lambda)] + \cosh[K(1-\lambda)]}{\cosh(K) + \frac{\delta\pi}{H_B}\sinh(K)}\right\} \tag{2-32}$$

and in the case $\lambda = 1$,

$$C_E(O) - C_E(L) = \frac{J_s}{\pi^2}\left[1 - \frac{1 + \frac{\delta\pi}{H_B}\sinh(K)}{\cosh(K) + \frac{\delta\pi}{H_B}\sinh(K)}\right] < \frac{J_s}{\pi^2}. \tag{2-33}$$

At least in the case of uniform solute pumps, the absence of perceptible gradients between the external bathing media at transport equilibrium rules out the presence of an intraepithelial gradient when transport is between identical media.

MODEL CALCULATIONS

The model Eqs. 2-2, 2-3, and 2-4 with boundary conditions in Eqs. 2-5, 2-6, and 2-8 were solved numerically for comparison with the analytical approximations. Because N is either constant or zero, Eq. 2-4 is integrated directly. The values for C_E and J_v are then obtained at $M + 1$ evenly spaced mesh points within the channel. To do this the differential Eqs. 2-2 and 2-3 are represented as $2M$ finite difference equations in the $2M + 2$ unknowns C_E^m and J_v^m where $m = 1, \ldots, M + 1$. The difference equations are centered in space so that, for example, Eq. 2-2 is represented by

$$\frac{1}{2}(J_s^m + J_s^{m+1}) = \frac{1}{2}(J_v^m + J_v^{m+1})\left[C_O + \frac{1}{2}(C_E^m + C_E^{m+1})\right] - DA\frac{(C_E^{m+1} - C_E^m)}{L/M}. \tag{3-1}$$

The boundary conditions in Eqs. 2-5 and 2-8 bring the equation count to $2M + 2$, the number of unknowns. This system of equations is solved iteratively using Newton's method. Approximately four to five significant digits were obtained using 21 mesh points ($M = 20$).

Table I lists a set of reference parameter values for the model calculations. $J_s = 3 \times 10^{-6}$ mosmol/s · cm^2 is taken to resemble a briskly transporting epithelium, such as rabbit gallbladder. Blom and Helander (1977) have made detailed morphologic observations of rabbit gallbladder and indicate that the channels occupy ~15% of epithelial volume, so we have set A = 0.15 cm^2/cm^2 epithelium. Further, they have indicated that the effective channel radius $r = 2A/S = 0.15 \times 10^{-4}$ cm, so that $S = 2 \times 10^4$ cm/cm^2 epithelium. The unit water permeability of the cell membrane was taken to be approximately that of the human red cell membrane, 2.2×10^{-4} cm/s.osmol, determined by Sha'afi et al. (1967). The reference solute permeability of the channel basement membrane, H_B, was set at 5×10^{-5} cm^3/s to obtain a strength of transport for this model of ~60 mosmol/liter. It may be noted that this permeability corresponds to an electrical resistance of 18 Ωcm^2. This resistance is comparable to the measured value of 11 Ωcm^2 for the subepithelial resistance of rabbit gallbladder

TABLE I
REFERENCE PARAMETERS

$J_s = 3.0 \times 10^{-6}$ mosmol/s · cm^2
$C_O = 0.3$ mosmol/cm^3
$\lambda = 1.0$
$A = 0.15$ cm^2/cm^2 epithelium
$S = 2.0 \times 10^4$ cm/cm^2 epithelium
$L = 5.0 \times 10^{-3}$ cm
$D = 1.0 \times 10^{-5}$ cm^2/s
$RTL_p = 2.0 \times 10^{-4} \dfrac{\text{cm}}{\text{s} \cdot (\text{mosmol/cm}^3)}$
$H_B = 5.0 \times 10^{-5}$ cm^3/s
$\pi = \sqrt{SLRTL_pC_O} = 7.7 \times 10^{-2}$
$\delta = \sqrt{\dfrac{DA}{L}} = 1.7 \times 10^{-2}$
$K = \dfrac{\pi}{\delta} = 4.5$

obtained by Henin et al. (1977), who pierced the epithelium from the mucosal side with microelectrodes. This resistance is, however, substantially higher than that suggested by the earlier work of Wright and Diamond (1968) and so we have included a complete set of calculations with $H_B = 1.25 \times 10^{-3}$ cm^3/s. The limited capacity for uphill transport with this value of H_B will be discussed below.

Fig. 2 displays the solution of the interspace model with the reference parameters for the case $C_M = C_S = O$. The three panels have a common abcissa, the fractional channel length, x/L. Numerical solution to the complete model Eqs. 2-2–2-4 has been indicated at the mesh points by "+"; the approximate analytical solution by solid curves. The upper panel is a graph of solute flux, $J_s(x)$, and shows the linear profile corresponding to uniform solute input along the interspace ($\lambda = 1$). The middle panel displays the interspace osmolality and indicates the small gradient from channel apex to base. The numerical model predicts $C_E(O) = 0.499$ mosmol/liter and $C_E(L) = 0.483$; the analytic estimate of these values is $C_E(O) = 0.500$ and $C_E(L) = 0.482$. The lowest panel shows $J_v(x)$ with $J_v(L) = (J_v)_0 = 9.912$ or 9.920 nl/s · cm^2 for numerical or analytical models. This corresponds to reabsorbate concentrations, $(C_R)_0 =$ 302.68 or 302.43 mosmol/liter so that $\gamma = 0.99$.

Figs. 3–6 may be viewed in conjunction with Tables II and III to understand the roles of the model parameters in defining the epithelial properties. The curves in each of these figures have been computed using the complete model equations. Figs. 3 *a*, 4 *a*, 5 *a*, and 6 *a* show simulations of strength of transport experiments. In each figure, transepithelial volume flow is plotted against mucosal bath osmolality for serosal bath osmolality fixed at the reference. The point of intersection of each curve with the line $J_v = 0$ gives the strength of transport, $\hat{C}$, for that particular parameter set. The intercepts have been determined by linear interpolation and have been listed in column 5 of Tables II and III (numerical solutions). Each of Figs. 3 *b*, 4 *b*, 5 *b*, and 6 *b* is composed of two panels: the left panel contains graphs of the transport tonicity, C_R, as the mucosal bath is varied below the reference osmolality; the right panel shows C_R as the serosal bath is increased above the reference. Each solid curve corresponds to

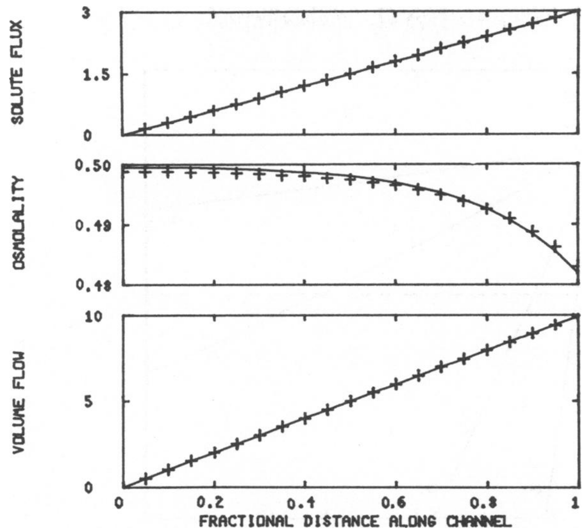

FIGURE 2 Interspace flux and osmolality profiles at level flow. The model equations have been solved using the reference parameters (Table I) and with bathing media of identical composition ($C_M = C_S = 0$). The numerical solution of the complete system is indicated by "+", the approximate analytical solution by a continuous curve. For each panel, the abcissa is fractional channel length. The upper panel shows solute flux (in nanosmol per second) and the lower panel, volume flow (in nanoliter per second); the middle panel is the increment of channel osmolality (milliosmol per liter) above reference.

a set of experiments for a given parameter set. In the left panels, the dashed line is the line of identity, $C_R = C_0 + C_M$, and the intersection of a solid curve with this line corresponds to a point of mucosal transport equilibrium. In the right panels, the dashed line is the graph of $C_R = C_0 + C_S$, and the intersection of a solid curve with this line corresponds to a point of serosal transport equilibrium. The equilibrium deviations, C_M^* and C_S^*, have been determined from these graphs by linear interpolation and are listed in columns 3 and 4 of Tables II and III (numerical solutions). The data from these experiments also include $J_v(C_M, O)$ and $J_v(O, C_S)$ for small values of C_M and C_S and hence permit the estimate of $-\partial J_v/\partial C_M$ (O, O) and $\partial J_v/\partial C_S$ (O, O). These water permeabilities have been listed in columns 6 and 7, along with their average in column 8 (Tables II and III-numerical solutions).

In the analytical solutions section of Tables II and III, $C_E(O)$ and $C_E(L)$ are computed according to Eqs. 2-20 and 2-21, $(J_v)_0$ and $(C_R)_0$ with Eq 2-22, $\hat{C}$ with Eq. 2-26, and $L_{P,\text{obs}}$ with Eq. 2-30. To compute the osmotic deviations for transport equilibrium, Eq. 2-22 was used to plot the transport tonicity as a function of the bath osmolality. The intersection of these curves with the line of slope equal to one was estimated by linear interpolation and is listed as C_M^* and C_S^* in columns 3 and 4 of Tables II and III (analytical solutions). The estimate of these deviations given by Eqs. 1-16 and 1-17 are listed in columns 5 and 6.

Fig. 3 is obtained using the reference parameters and three additional values of H_B that span two orders of magnitude. The strength of transport is crucially dependent upon H_B (Fig. 3 *a*) although transport isotonicity is little influenced by this parameter (Fig. 3 *b*). As may be seen in Fig. 3 *a*, H_B strongly affects the slope of $J_v(C_M, O)$, and is, therefore, a major

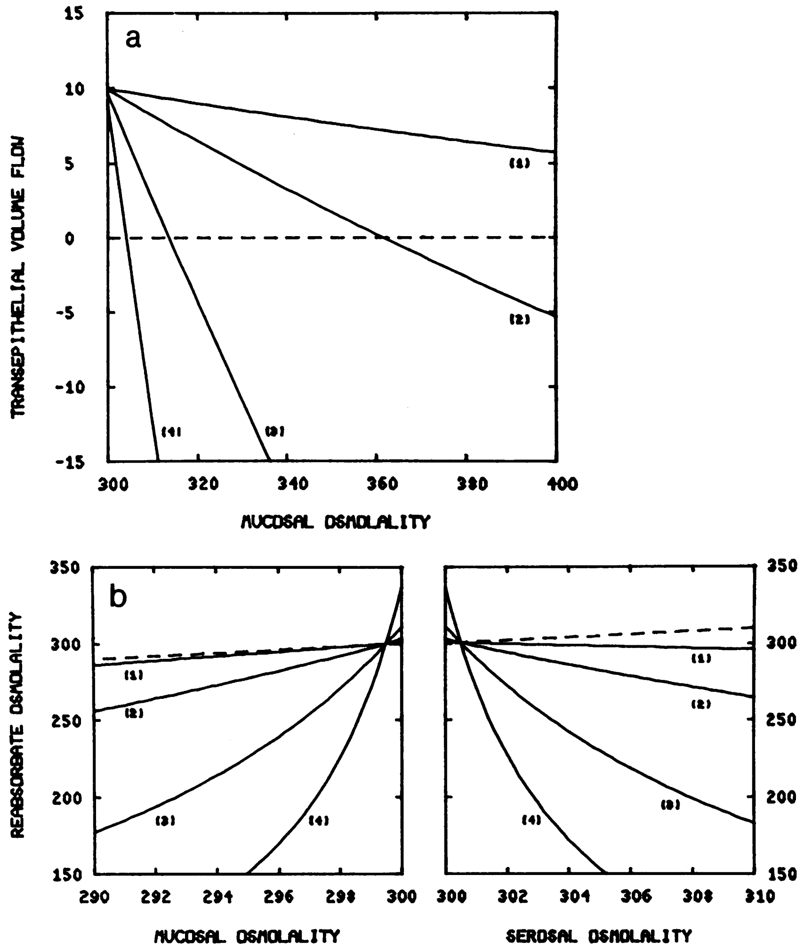

FIGURE 3 (*a*) Volume flow against an adverse osmotic gradient: effect of basement membrane solute permeability. Transepithelial volume flow (nanoliter per second), determined by the numerical solution of the complete model equations is plotted as a function of mucosal bath osmolality. The fixed model parameters are taken at their reference values (Table I) and the four curves are determined by varying the basement membrane solute permeability: (1) $H_B = 10^{-6}$ cm^3/s, (2) $H_B = 0.5 \times 10^{-5}$ cm^3/s, (3) $H_B = 2.5 \times 10^{-5}$ cm^3/s, (4) $H_B = 1.25 \times 10^{-4}$ cm^3/s. The dashed line is the line of zero volume flow and its intersection with any of the curves shows the strength of transport, $\hat{C}$, for that parameter set. (*b*) Transport tonicity as a function of bath osmolality and the condition of transport equilibrium: effect of basement membrane solute permeability. In the left panel the osmolality of the transported solution, C_R, as determined by the numerical solution of the model equations, is plotted as a function of the mucosal bath osmolality when the serosal bath is held at the reference. In the right panel, C_R is a function of serosal osmolality while the mucosa is at reference. The parameters determining the four curves are as in Fig. 3 *a*. In the left panel the dashed line is the line of identity, $C_R = C_O + C_M$, and the intersection with any of the curves occurs at the point of mucosal transport equilibrium, $C_0 + C_M^*$. In the right panel the dashed line is given by $C_R = C_O + C_S$, and the intersection with any of the curves occurs at the point of serosal transport equilibrium, $C_O + C_S^*$.

TABLE II

NUMERICAL AND ANALYTIC SOLUTIONS

Numerical solutions	Parameters									
	$(J_v)_O$	$(C_R)_O$	C^*_M	C^*_S	$\hat{C}$	$\frac{-\partial J_v}{\partial C_M}$	$\frac{\partial J_v}{\partial C_S}$	$L_{P,obs}$	$C_E(O)$	$C_E(L)$
	nl/s · cm²		*mosmol/liter*			*cm × 10⁴/s · osmol*			*mosmol/liter*	
$D \times 0.04$	9.922	302.37	0.635	0.499	69.71	1.57	1.24	1.41	0.499	0.429
$D \times 0.2$	9.915	302.58	0.622	0.499	64.13	1.70	1.37	1.54	0.499	0.465
Reference	9.912	302.68	0.616	0.499	61.62	1.77	1.44	1.60	0.499	0.483
$D \times 5.0$	9.910	302.73	0.614	0.499	60.52	1.80	1.47	1.64	0.497	0.492
$L_P \times 0.04$	8.230	364.54	16.549	12.019	63.14	1.40	1.17	1.29	10.513	9.815
$L_P \times 0.1$	9.199	326.14	6.334	4.920	62.90	1.59	1.31	1.45	4.688	4.404
$L_P \times 0.2$	9.580	313.17	3.123	2.480	62.59	1.68	1.37	1.52	2.433	2.302
Reference	9.912	302.68	0.616	0.499	61.62	1.77	1.44	1.60	0.499	0.483
$L_P \times 5.0$	9.982	300.54	0.123	0.100	60.83	1.81	1.47	1.64	0.100	0.098
$H_B \times 0.2$	9.975	300.75	1.527	0.499	301.33	0.50	0.16	0.33	0.499	0.497
Reference	9.912	302.68	0.616	0.499	61.62	1.77	1.44	1.60	0.499	0.483
$H_B \times 5.0$	9.641	311.16	0.525	0.500	13.71	7.17	6.86	7.01	0.497	0.422
$H_B \times 25.0$	8.915	336.50	0.510	0.501	4.13	21.69	21.40	21.55	0.494	0.259

Analytic solutions	$(J_v)_O$	$(C_R)_O$	C^*_M	C^*_S	C^*_M-est	C^*_S-est	$\hat{C}$	$L_{P,obs}$‡	$C_E(O)$	$C_E(L)$
	nl/s · cm²				*mosmol/liter*					
$D \times 0.04$	9.930	302.12	0.656	0.404	0.654	0.405	70.68	1.40	0.500	0.421
$D \times 0.2$	9.923	302.33	0.639	0.411	0.637	0.412	64.50	1.54	0.500	0.462
Reference	9.920	302.43	0.631	0.414	0.630	0.415	61.74	1.61	0.500	0.482
$D \times 5.0$	9.918	302.48	0.628	0.416	0.626	0.416	60.54	1.64	0.498	0.492
$L_P \times 0.04$	8.348	359.37	17.064	10.048	15.834	10.326	63.17	1.32	10.687	9.912
$L_P \times 0.1$	9.264	323.83	6.507	4.087	6.328	4.133	62.96	1.47	4.731	4.414
$L_P \times 0.2$	9.616	311.96	3.204	2.056	3.160	2.068	62.69	1.53	2.447	2.301
Reference	9.920	302.43	0.631	0.414	0.630	0.415	61.74	1.61	0.500	0.482
$L_P \times 5.0$	9.984	300.49	0.126	0.083	0.125	0.083	60.90	1.64	0.100	0.098
$H_B \times 0.2$	9.983	300.50	0.***	0.249	0.***	0.249	301.74	0.33	0.500	0.496
Reference	9.920	302.43	0.631	0.414	0.630	0.415	61.74	1.61	0.500	0.482
$H_B \times 5.0$	9.649	310.92	0.526	0.478	0.524	0.478	13.74	7.02	0.498	0.421
$H_B \times 25.0$	8.922	336.26	0.510	0.495	0.507	0.493	4.14	21.57	0.494	0.259

*As in Table I.

‡Units ($L_{P,obs}$) cm × 10^4 s · osmol.

determinant of $L_{P,obs}$. With reference to Table II, $L_{P,obs}$ varies by a factor of 65 with the 125-fold change in H_B. It is of interest to note that with the reference value of H_B the value of $RTL_{P,obs}$, 1.6×10^{-4} cm³/s · osmol, is comparable to that measured by Van Os et al. (1979), 1.7×10^{-4} cm³/s · osmol, before they corrected for solute polarization. Fig. 4 is obtained using the reference parameters and three additional values of L_P. In this case, neither strength of transport nor $L_{P,obs}$ seems to be much influenced by L_P (Fig. 4 *a*) although C^*_M and C^*_S are quite sensitive to this parameter (Fig. 4 *b*). Table II shows that as L_P varies by a factor of 125, $L_{P,obs}$ varies by only a factor of 1.3. Table II also indicates that near this reference parameter

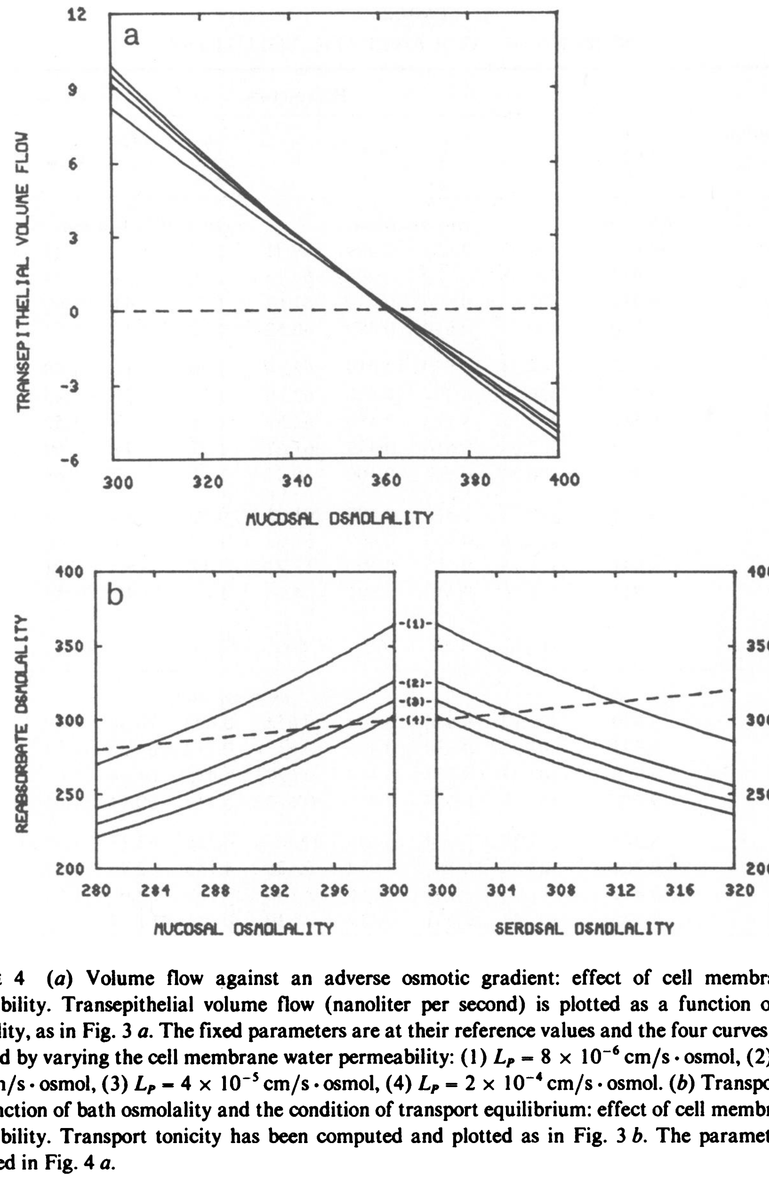

FIGURE 4 (*a*) Volume flow against an adverse osmotic gradient: effect of cell membrane water permeability. Transepithelial volume flow (nanoliter per second) is plotted as a function of mucosal osmolality, as in Fig. 3 *a*. The fixed parameters are at their reference values and the four curves have been obtained by varying the cell membrane water permeability: (1) $L_P = 8 \times 10^{-6}$ cm/s · osmol, (2) $L_P = 2 \times 10^{-5}$ cm/s · osmol, (3) $L_P = 4 \times 10^{-5}$ cm/s · osmol, (4) $L_P = 2 \times 10^{-4}$ cm/s · osmol. (*b*) Transport tonicity as a function of bath osmolality and the condition of transport equilibrium: effect of cell membrane water permeability. Transport tonicity has been computed and plotted as in Fig. 3 *b*. The parameters are as indicated in Fig. 4 *a*.

set, changes in the diffusion coefficient have little effect on strength of transport, transport isotonicity, or $L_{P,\mathrm{obs}}$.

In computing Figs. 5 and 6 and Table III, the basement membrane solute permeability was set at 25 times the reference. This was done to display to better advantage the performance of a model in which the standing gradient features are dominant as well as to consider a basement membrane resistance more compatible with the estimate of Wright and Diamond (1968). Table III shows that with this higher basement membrane solute permeability the transport tonicity between equal bathing media, $(C_R)_O$, equals 336.5 mosmol/liter corre-

TABLE III

NUMERICAL AND ANALYTIC SOLUTIONS: HIGH BASEMENT MEMBRANE SOLUTE PERMEABILITY

Numerical solutions	Parameters									
	$(J_v)_O$	$(C_R)_O$	C_M^*	C_S^*	$\hat{C}$	$\dfrac{-\partial J_v}{\partial C_M}$	$\dfrac{\partial J_v}{\partial C_S}$	$L_{P,obs}$	C_E (O)	C_E (L)
$H_B \times 25.0$;	*nl/s · cm²*		*mosmol/liter*			*cm × 10⁴/s · osmol*			*mosmol/liter*	
$D \times 0.04$	9.624	311.72	0.524	0.500	12.93	7.52	7.20	7.36	0.499	0.090
$D \times 0.2$	9.317	321.99	0.514	0.501	6.86	13.65	13.35	13.50	0.499	0.163
$D \times 1.0$	8.915	336.50	0.510	0.501	4.13	21.69	21.40	21.55	0.494	0.259
$D \times 5.0$	8.540	351.29	0.509	0.502	2.94	29.19	28.93	29.06	0.460	0.349
$L_p \times 0.04$	3.074	975.93	13.351	12.020	5.56	5.53	5.50	5.51	4.892	1.660
$L_p \times 0.1$	5.160	581.43	5.181	4.920	5.35	9.66	9.56	9.61	3.225	1.159
$L_p \times 0.2$	6.690	448.41	2.566	2.481	5.08	13.22	13.06	13.14	2.039	0.792
$L_p \times 1.0$	8.915	336.50	0.510	0.501	4.13	21.69	21.40	21.55	0.494	0.259
$L_p \times 5.0$	9.704	309.14	0.104	0.103	3.30	29.57	29.24	29.40	0.100	0.071
$D \times 0.04$; $L_p \times 0.04$	7.732	387.98	15.472	12.019	44.14	1.80	1.59	1.69	11.831	0.543
$D \times 0.04$; $L_p \times 0.1$	8.613	348.32	5.695	4.920	31.80	2.77	2.50	2.64	4.914	0.332
$D \times 0.04$; $L_p \times 0.2$	9.053	331.39	2.743	2.480	24.33	3.78	3.50	3.64	2.479	0.227
$D \times 0.04$; $L_p \times 1.0$	9.624	311.72	0.524	0.500	12.93	7.52	7.20	7.36	0.499	0.090
$D \times 0.04$; $L_p \times 5.0$	9.863	304.16	0.104	0.101	7.26	13.68	13.35	13.51	0.100	0.033
Analytic solutions	$(J_v)_O$	$(C_R)_O$	C_M^*	C_S^*	C_M^*-est	C_S^*-est	$\hat{C}$	$L_{P,obs}$‡	$C_E(O)$	$C_E(L)$
$H_B \times 25.0$;	*nl/s · cm²*				*mosmol/liter*					
$D \times 0.04$	9.632	311.47	0.524	0.479	0.523	0.479	13.08	7.36	0.500	0.088
$D \times 0.2$	9.324	321.74	0.514	0.489	0.512	0.489	6.90	13.51	0.500	0.162
$D \times 1.0$	8.922	336.26	0.510	0.495	0.507	0.493	4.14	21.57	0.494	0.259
$D \times 5.0$	8.545	351.07	0.509	0.497	0.505	0.495	2.94	29.09	0.460	0.349
$L_p \times 0.04$	3.082	973.48	13.354	11.824	12.736	12.272	5.57	5.53	4.906	1.660
$L_p \times 0.1$	5.173	579.88	5.182	4.836	5.091	4.912	5.36	9.65	3.236	1.158
$L_p \times 0.2$	6.705	447.45	2.566	2.440	2.543	2.458	5.09	13.18	2.046	0.791
$L_p \times 1.0$	8.922	336.26	0.510	0.495	0.507	0.493	4.14	21.57	0.494	0.259
$L_p \times 5.0$	9.706	309.09	0.104	0.102	0.101	0.099	3.30	29.41	0.100	0.071
$D \times 0.04$; $L_p \times 0.04$	7.857	381.85	15.730	10.527	14.753	10.844	45.82	1.71	12.226	0.514
$D \times 0.04$; $L_p \times 0.1$	8.676	345.79	5.736	4.449	5.613	4.508	32.76	2.65	4.992	0.318
$D \times 0.04$; $L_p \times 0.2$	9.088	330.12	2.754	2.293	2.726	2.308	24.90	3.65	2.500	0.219
$D \times 0.04$; $L_p \times 1.0$	9.632	311.47	0.524	0.479	0.523	0.479	13.08	7.36	0.500	0.088
$D \times 0.04$; $L_p \times 5.0$	9.865	304.11	0.104	0.099	0.102	0.098	7.30	13.51	0.100	0.032

*As in Table I.

‡Units ($L_{P,obs}$) cm × 10⁴/s · osmol.

sponding to a coupling coefficient, $\gamma = 0.89$. Nevertheless, the model transports isotonically with $C_M^* = 0.51$ mosmol/liter and $C_S^* = 0.50$ mosmol/liter. These calculations underscore the point that the simple calculation of $(C_R)_O$ is not by itself sufficient to decide the issue of transport isotonicity.

Fig. 5 contains curves obtained using three additional values of the diffusion coefficient (or, equivalently, the channel cross-section, A) that span two orders of magnitude. Fig. 5 *a* shows

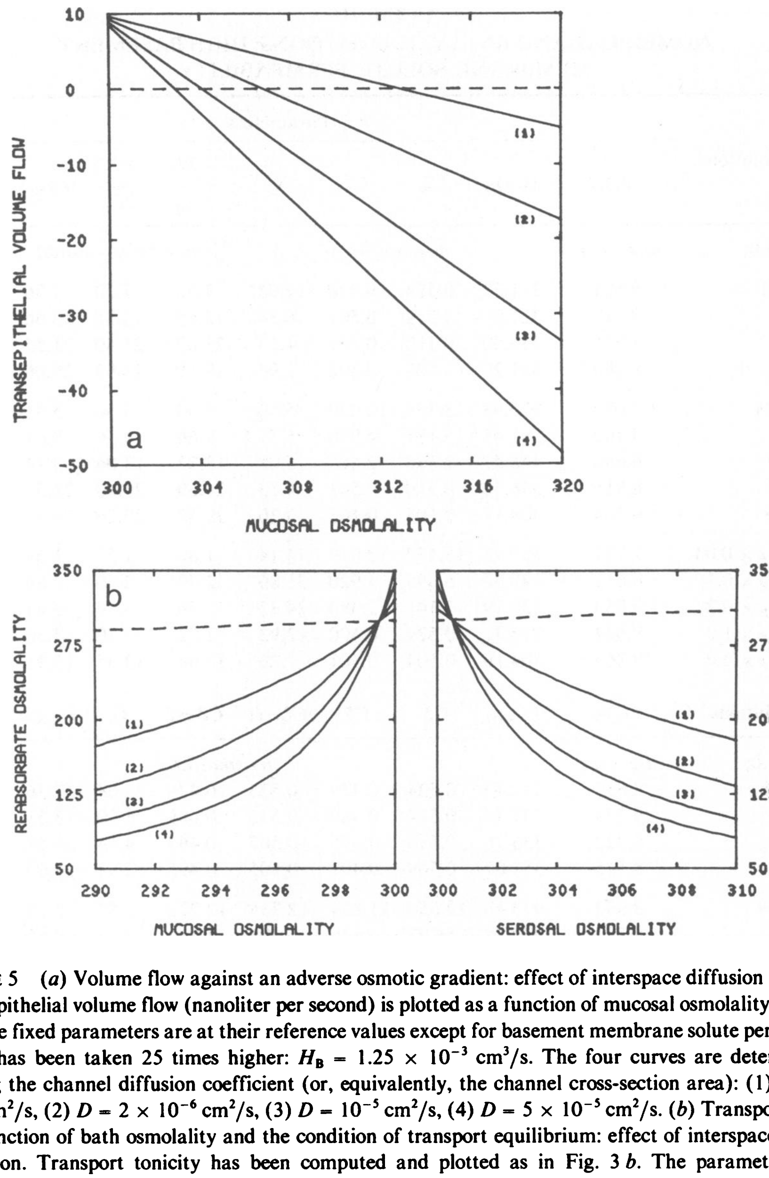

FIGURE 5 (*a*) Volume flow against an adverse osmotic gradient: effect of interspace diffusion limitation. Transepithelial volume flow (nanoliter per second) is plotted as a function of mucosal osmolality, as in Fig. 3 *a*. The fixed parameters are at their reference values except for basement membrane solute permeability, which has been taken 25 times higher: $H_B = 1.25 \times 10^{-3}$ cm³/s. The four curves are determined by varying the channel diffusion coefficient (or, equivalently, the channel cross-section area): (1) $D = 4 \times 10^{-7}$ cm²/s, (2) $D = 2 \times 10^{-6}$ cm²/s, (3) $D = 10^{-5}$ cm²/s, (4) $D = 5 \times 10^{-5}$ cm²/s. (*b*) Transport tonicity as a function of bath osmolality and the condition of transport equilibrium: effect of interspace diffusion limitation. Transport tonicity has been computed and plotted as in Fig. 3 *b*. The parameters are as indicated in Fig. 5 *a*.

that the strength of transport and effective water permeability in this model are quite sensitive to the diffusion limitation within the channel. In Fig. 5 *b* one sees that the diffusion coefficient plays virtually no role in the achievement of isotonic transport. It is a serious problem for this model, however, that even for a diffusion coefficient 1/25 of the reference, the strength of transport is only 12.9 mosmol/liter.

The influence of cell membrane water permeability in limiting the ability of a standing gradient system to transport against an adverse osmotic gradient is illustrated in Fig. 6. For this figure, the diffusion coefficient has been kept at 1/25 of the reference value to further enhance the effect on strength of transport. Fig. 6 has been computed for the same cell membrane water permeabilities that were used in Fig. 4. In contrast to Fig. 4 *a*, however, Fig. 6 *a* shows both the strength of transport and effective water permeability, to be sensitive to changes in L_P in this predominantely standing gradient model. The constraint on cell membrane water permeability imposed by isotonic transport is recalled by Fig. 6 *b* where it is seen that if L_P is diminished to enhance transport strength, isotonicity may be compromised (Table III).

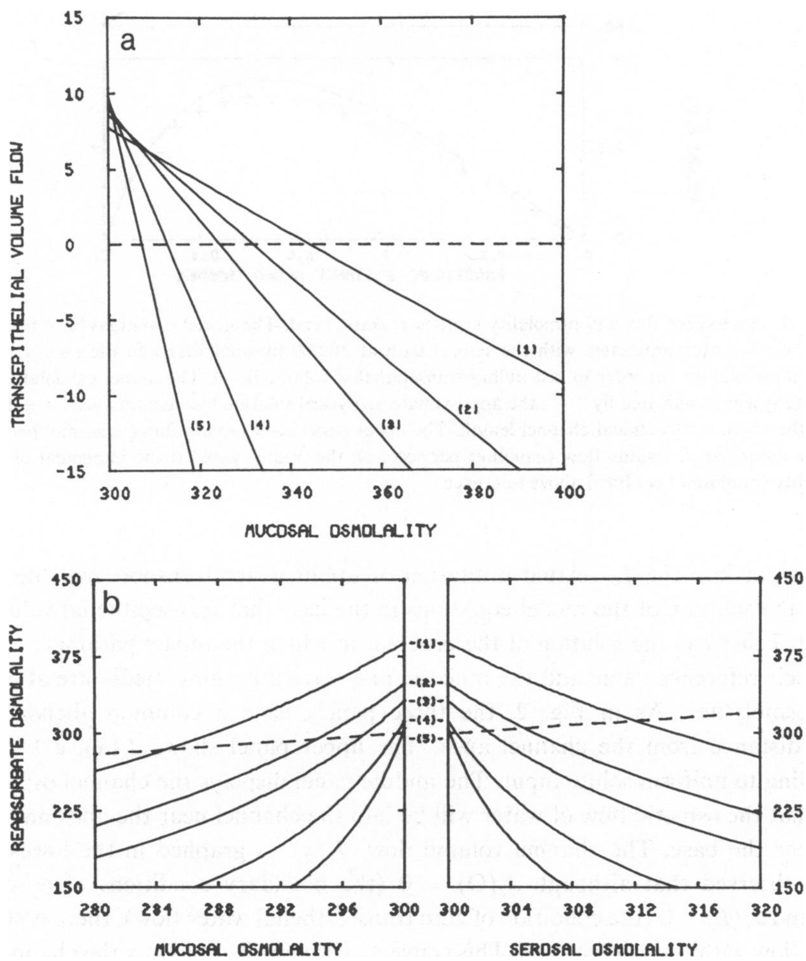

FIGURE 6 (*a*) Volume flow against an adverse osmotic gradient: effect of cell membrane water permeability. Transepithelial volume flow (nanoliter per second) is plotted as a function of mucosal osmolality as in Fig. 3 *a*. The fixed parameters are at their reference values except for basement membrane solute permeability, which is 25 times higher. (H_B = 1.25 × 10^{-3} cm^3/s) and the channel diffusion coefficient, which is 25 times smaller (D = 4 × 10^{-7} cm^2/s). The five curves have been obtained by varying the cell membrane water permeability: (1) L_P = 8 × 10^{-6} cm/s · osmol, (2) L_P = 2 × 10^{-5} cm/s · osmol, (3) L_P = 4 × 10^{-5} cm/s · osmol, (4) L_P = 2 × 10^{-4} cm/s · osmol, (5) L_P = 10^{-3} cm/s · osmol. (*b*) Transport tonicity as a function of bath osmolality and the condition of transport equilibrium: effect of cell membrane water permeability. Transport tonicity has been computed and plotted as in Fig. 3 *b*. The parameters are as indicated in Fig. 6 *a*.

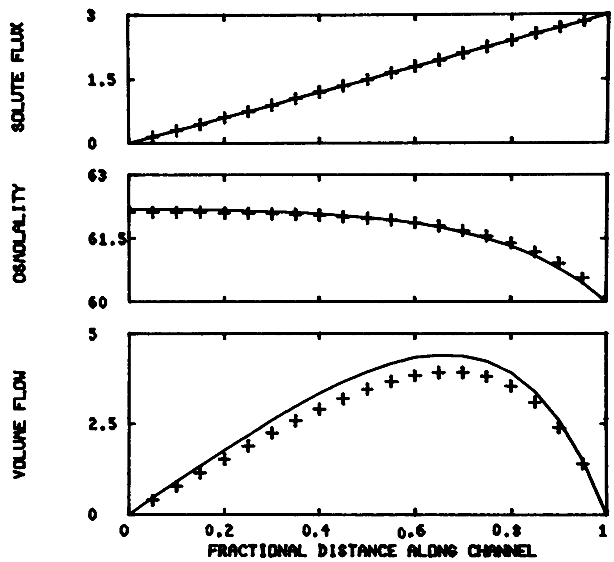

FIGURE 7 Interspace flux and osmolality profiles at static head. The model equations have been solved using the reference parameters with the serosal bath at 300.00 mosmol/liter and the mucosal bath at 361.74 mosmol/liter (in order to just nullify transepithelial volume flow). The numerical solution of the complete sysem is indicated by "+", the approximate analytical solution by a continuous curve. For each panel, the abcissa is fractional channel length. The upper panel shows solute flux (nanosmol per second) and the lower panel, volume flow (nanoliter per second); the middle panel is the increment of channel osmolality (milliosmol per liter) above reference.

Some insight into the L_p-related limitation of uphill water transport may be gained by examining the solution of the model equations in the case that transepithelial volume flow is nulled. Fig. 7 displays the solution of the problem in which the model parameters have been taken at their reference value and the mucosal and serosal bathing media are at 361.74 and 300.00 mosmol/liter. As in Fig. 2, the three panels have a common abcissa, x/L, the fractional distance from the channel apex. The upper panel shows $J_s(x)$, a linear profile corresponding to uniform solute input. The middle panel displays the channel osmolality and indicates that the osmotic flow of water will be into the channel near the apex and out of the channel near the base. The channel volume flow, $J_v(x)$, is graphed in the lowest panel. It should be observed that although $J_v(O) = 0$ (the boundary conditions of a sealed tight junction) and $J_v(L) = 0$ (the condition of zero transepithelial water flow), there is still positive convective flow within the interspace. This convective flow will act to mix the channel contents and mitigate the diffusion limitation of solute flux.

The capacity for uphill transport in a standing gradient model with uniform solute pumps may be addressed directly by considering Eq. 2-27. If one supposes that the basement membrane effect is negligible then

$$\hat{C} \approx \frac{J_s}{\delta\pi}\left[\frac{1}{\tanh(K)} - \frac{1}{K}\right] \leq \frac{J_s}{\delta\pi} \tag{3-2}$$

and by using Eq. 2-29 to eliminate π, one obtains

$$\hat{C} \leq \left[\frac{C^* J_s L}{DA}\right]^{1/2}. \tag{3-3}$$

Each of the symbols in Eq. 3-3 represents a measurable quantity. For rabbit gallbladder we shall use $J_s = 4.2 \times 10^{-6}$ mosmol/s · cm^2 (Diamond, 1964 *a*) and $A = 0.15$ cm^2/cm^2 epithelium (Blom and Helander, 1977). If one supposes that transport is isotonic to within 2%, then $C^* = 6.0 \times 10^{-3}$ mosmol/cm^3. For a diffusion coefficient $D = 1.5 \times 10^{-5}$ cm^2/s and channel length $L = 0.005$ cm, Eq. 3-3 gives the estimate $\hat{C} \leq 7.5$ mosmol/liter. This is approximately one order of magnitude less than the measured value of 80 mosmol/liter (Diamond, 1964 *a*). It appears doubtful, therefore, that the classical standing gradient interspace model is adequate to represent the uphill transport properties of this epithelium.

CONCLUSION

The intuitive notions of coupled water transport have developed along with experimental familiarity with such tissues as rabbit gallbladder or dog small intestine that can transport both isotonically and against an osmotic gradient. Mathematical models of these epithelia have been devised to understand the tissue physiology in terms of the transport laws for simple membranes. The adequacy of such composite systems will be judged both by their simulation of experimental observation and by the correspondence of the model components to the known epithelial structures.

In this paper, we have outlined in a general way a minimal set of calculations necessary to assess the osmotic performance of a model. What is required is a series of calculations of transepithelial solute and volume flux for a range of bathing solution osmolalities in order to determine the strength of transport for the model, its effective water permeability, and the conditions for mucosal and serosal transport equilibrium. In this last case one identifies the bath conditions in which the transported solution is isosmotic to one of the two bathing media. The calculation of the transport tonicity for the case of identical bathing solutions $(C_R)_0$, while not an experimentally observed quantity, does provide a useful measure of intraepithelial coupling, $\gamma = C_0/(C_R)_0$.

From any general model of epithelial transport, a linear model may be obtained simply by taking the early terms of the Taylor series for the transepithelial flux relations. The use of γ as a measure of coupling is given support by the observation in the approximate model that, taken together, uphill water transport and isotonic transport imply that coupling is tight ($\gamma \approx 1.$). With this formulation, one defines a virtual volume flow that is relevant to transport isotonicity, $(J_s)_0/C_0$. The coupled volume flow, $(J_v)_0 = \gamma[(J_s)_0/C_0]$, is that which occurs between identical bathing media. The noncoupled fraction, $C^* L_{P,\mathrm{obs}} = (1 - \gamma)[(J_s)_0/C_0]$ must be driven by the establishment of a transepithelial osmotic gradient, whose magnitude depends upon the tissue water permeability. Several important epithelial models are of just the form to which this analysis applies.

A model of the lateral interspace has been presented that combines features of both the compartment type and standing gradient models. The isotonic convection approximation of

Segel has been used to obtain analytic estimates of the transepithelial fluxes and intraepithelial concentrations as a function of the bath osmolalities. It is shown that the condition of isotonic transport depends critically on the water permeability of the cell membrane and is little influenced by basement membrane solute permeability or the diffusion limitation of solute movement within the interspace. It is also shown that with a tightly coupled epithelium, the measured water permeability is only a fraction $(1 - \gamma)$ of the permeability relevant to isotonicity. This discrepancy is an inescapable feature of intraepithelial solute-solvent coupling.

The strength of transport for this model is displayed as the sum of two terms. The first term is simply that for a well-stirred compartment model and reflects basement membrane solute permeability. The second term measures the added strength due to diffusion limitation within the interspace. This is the first analytical estimate of the strength of transport of a standing gradient system. An important observation from this estimate is that the capacity for uphill transport by a purely standing gradient model may be severely compromised by the high cell membrane water permeability necessary for transport isotonicity.

A series of numerical calculations that solve the nonlinear model equations exactly shows the analytical estimates to be of useful accuracy. Further, it appears that with the appropriate choice of parameters, the osmotic character of an epithelium such as rabbit gallbladder can be adequately simulated. With these simulations it is found that neither the strength of transport nor the achievement of isotonic transport is much influenced by intraepithelial diffusion. Thus, it seems likely that with respect to questions of coupled water transport, the basic compartmental scheme of Curran should continue to provide satisfactory answers.

Received for publication 6 August 1980 and in revised form 17 March 1981.

REFERENCES

Blom, H., and H. F. Helander. 1977. Quantitative electron microscopical studies on in vitro incubated rabbit gallbladder epithelium. *J. Membr. Biol.* 37:45–61.

Curran, P. F. 1960. Na, Cl, and water transport by rat ileum in vitro. *J. Gen. Physiol.* 43:1137–1148.

Curran, P. F., and J. R. MacIntosh. 1962. A model system for biological water transport. *Nature (Lond.)* 193:347–348.

Currant, P. F., and A. K. Solomon. 1957. Ion and water fluxes in the ileum of rats. *J. Gen. Physiol.* 41:143–168.

Diamond, J. M. 1964 *a*. Transport of salt and water in rabbit and guinea pig gall bladder. *J. Gen. Physiol.* 48:1–14.

Diamond, J. M. 1964 *b*. The mechanism of isotonic water transport. *J. Gen. Physiol.* 48:15–42.

Diamond, J. M. 1966. Non-linear osmosis. *J. Physiol. (Lond.).* 183:58–82.

Diamond, J. M. 1978. Solute-linked water transport in epithelia. *In* Membrane Transport Processes. J. F. Hoffman, editor. Raven Press, New York. 257–276.

Diamond, J. M. 1979. Osmotic water flow in leaky epithelia. *J. Membr. Biol.* 51:195–216.

Diamond, J. M., and W. H. Bossert. 1967. Standing-gradient osmotic flow. A mechanism for coupling of water and solute transport in epithelia. *J. Gen. Physiol.* 50:2061–2083.

DiBona, D. R., and J. W. Mills. 1979. Distribution of Na^+-pump sites in transporting epithelia. *Fed. Proc.* 38:134–143.

Henin, S., D. Cremaschi, T. Schettino, G. Meyer, C. L. L. Donin, and F. Cotelli. 1977. Electrical parameters in gallbladders of different species. Their contribution to the origin of the transmural potential difference. *J. Membr. Biol.* 34:73–91.

Hill, A. E. 1975. Solute-solvent coupling in epithelia: a critical examination of the standing-gradient osmotic flow theory. *Proc. R. Soc. Lond. Biol. Sci.* 190:99–114.

Hill, A. E. 1977. General mechanisms of salt-water coupling in epithelia. *In* Transport of Ions and Water in Animals. B. Gupta, R. Moreton, J. Oschman, and B. Wall, editors. Academic Press, Inc., New York. 183–214.

Hill, B. S., and A. E. Hill. 1978. Fluid transfer by Necturus gall bladder epithelium as a function of osmolarity. *Proc. R. Soc. Lond. Biol Sci.* 200:151–162.

Huss, R. E., and D. J. Marsh. 1975. A model of NaCl and water flow through paracellular pathways of renal proximal tubules. *J. Membr. Biol.* 23:305–347.

Kyte, J. 1976. Immunoferritin determination of the distribution of ($Na^+ + K^+$) ATPase over the plasma membranes of renal convoluted tubules. II. Proximal segment. *J. Cell Biol.* 68:304–318.

Lin, C. C., and L. A. Segel. 1974. Illustration of techniques on a physiological flow problem. *In* Mathematics applied to Deterministic Problems in the Natural Sciences. Macmillan, Inc., New York. 244–276.

Ogilvie, J. T., J. R. MacIntosh, and P. F. Curran. 1963. Volume flow in a series-membrane system. *Biophys. Acta.* 66:441–444.

Sackin, H., and E. L. Boulpaep. 1975. Models for coupling of salt and water transport. Proximal tubular reabsorption in Necturus kidney. *J. Gen. Physiol.* 66:671–733.

Segel, L. A. 1970. Standing-gradient flows driven by active solute transport. *J. Theor. Biol.* 29:233–250.

Sha'afi, R. I., G. T. Rich, V. W. Sidel, W. Bossert, and A. K. Solomon. 1967. The effect of the unstirred layer on human red cell water permeability. *J. Gen. Physiol.* 50:1377–1399.

Stirling, C. E. 1972. Radioautographic localization of sodium pump sites in rabbit intestine. *J. Cell Biol.* 53:704–714.

van Os, C. H., G. Wiedner, and E. M. Wright. 1979. Volume flows across gallbladder epithelium induced by small hydrostatic and osmotic gradients. *J. Membr. Biol.* 49:1–20.

Weinstein, A. M., and J. L. Stephenson. 1979. Electrolyte transport across a simple epithelium. Steady-state and transient analysis. *Biophys. J.* 27:165–186.

Whitlock, R. T., and H. O. Wheeler. 1964. Coupled transport of solute and water across rabbit gallbladder epithelium. *J. Clin. Invest.* 48:2249–2265.

Wright, E. M., and J. M. Diamond. 1968. Effects of pH and polyvalent cations on the selective permeability of gall-bladder epithelium to monovalent ions. *Biochim. Biophys. Acta.* 163:57–74.